2D and 3D Simulation of Ductile Crack Propagation by Plastic Collapse of Micro-ligaments

Geralf Hütter*, Lutz Zybell, Uwe Mühlich and Meinhard Kuna

TU Bergakademie Freiberg, Institute of Mechanics and Fluid Dynamics, Lampadiusstr. 4, 09596 Freiberg, Germany

*geralf.huetter@imfd.tu-freiberg.de

Keywords: fracture mechanics, ductile crack growth, FEM simulation, micromechanics

Abstract. Numerical simulations of ductile crack growth are performed with a micro-mechanical model where discrete voids are incorporated near the crack tip. In contrast to previous studies the voids are assumed to be distributed uniformly in the whole domain. Numerous regularly arranged voids are resolved discretely near the crack tip where steep gradients occur whereas the voids are taken into account in a homogenized way by the GTN-model anywhere else. Cylindrical and spherical voids are considered. The results show that no damage of the intervoid ligaments is necessary for crack propagation but that the geometric softening is sufficient to induce a continuous shift of the currently active softening zone. Due to this mechanism a global limit load exists corresponding to the maximum crack growth resistance. The shielding effect due to the void growth in the plastic zone is highlighted.

Introduction

In the range of room temperature typical engineering metals fail by a ductile mechanism. In this process, particles debond from the embedding metallic matrix. The voids generated thereby grow and coalesce finally resulting in a macroscopic crack. The volume fractions of the particle differs in typical engineering metals and reach from considerably below 1% in steels up to more than 10% in ductile cast iron. The ductile failure mechanism has been the subject of numerous experimental and theoretical studies. For an overview see e.g. [1].

In the theoretical field two main approaches were pursued. The first one is related to the behavior of a unit cell. The analytical limit load analysis of Gurson [2] belongs to this class as well as the computational cell models used e.g. by Tvergaard [3-4] to extend the original Gurson model. Many other studies of the latter type could by listed. Tvergaard [3-4] found that macroscopic softening can occur despite stable deformation of the intervoid matrix material.

Models of the second type deal with the behavior of voids near an a-priori existent crack tip. The big computational effort restricted the first investigations to post-processing operations on the results for compact material [5-6]. The increasing computing facilities allowed to incorporate a single discrete void [7-9] up to several ones [10-15].

In [12-14] a critical reduction ratio of the respective first micro-ligament was employed. Having reached this value the micro-ligament was assumed to be failed and thus separated completely. A node-release technique allowed to simulate the crack propagation numerically. An influence of the critical value of the reduction ratio was noticed. However, as known from the cell model simulations material separation is not necessary for softening to occur.

In all studies [7-15] containing an a-priori crack the material outside the discrete void region was modeled identically to the matrix material. This approach is inconsistent insofar as the homogenized macroscopic material should differ from those of the matrix due to the presence of the voids.

In the present study discrete voids are incorporated in the numerical model near the crack tip. The material around this zone of discrete voids is consistently described in a homogenized way by the GTN-model. The homogenized model allows an adequate description only in those regions where no relevant gradients occur over two neighboring voids. Hence, a large number of voids is resolved discretely in order to be able to simulate sufficient crack growth.

Model

Mode I crack propagation for a semi-infinite crack is considered implying small-scale yielding. Plane strain conditions and isotropic material behavior are assumed.

The far-field is given by the K-solution with the stress intensity factor K_I and the corresponding energy-release rate

$$J = \frac{K_I^2(1-\nu^2)}{E} \quad . \tag{1}$$

Therein, the terms E and ν denote Young's modulus and Poisson ratio. Voids are assumed to be equally distributed in the material. Directly at the crack tip the cylindrical respectively spherical voids are resolved discretely whereas they are taken into account in a homogenized way by means of the GTN-model outside the process zone. The latter is well-known and not repeated here. The pa-

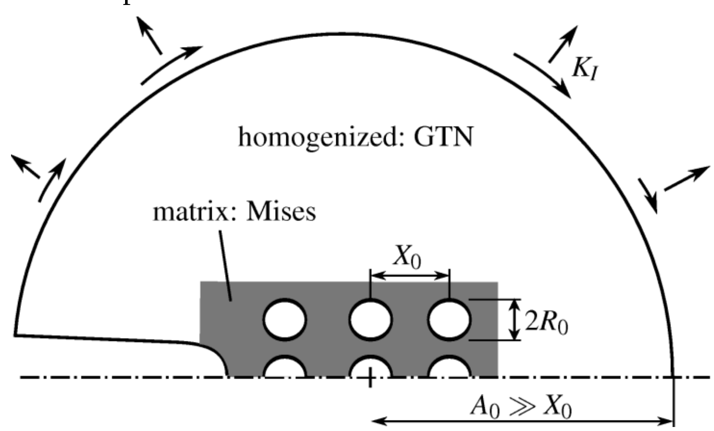

Fig. 1: Semi-infinite crack with discretely resolved process zone

rameters q_1=1.5 and q_2=1 are used as proposed in [3-4] for both shapes of voids. Due to symmetry only a half-model needs to be considered as sketched in Fig. 1. The material between the voids is described by Mises-plasticity with a hardening law given implicitly by

$$\sigma_\mathrm{y} = \sigma_0 \left(\frac{E\varepsilon_\mathrm{peq}}{\sigma_0} - \frac{\sigma}{\sigma_0} \right)^N \quad \text{for} \quad \sigma_\mathrm{y} \geq \sigma_0 \tag{2}$$

for the relation between equivalent plastic strain ε_peq and yield stress σ_y. The symbol σ_0 denotes the initial yield stress and N is the hardening exponent. The used values σ_0/E=0.003, N=0.1 and ν=0.3 are representative for typical medium strength engineering metals.

In the following finite element simulations, two types of void representations are investigated. In a first step a plane model with circular holes is considered corresponding to cylindrical voids. In a second step a more realistic model with spherical voids is studied which is, however, computationally much more expensive. Both types of void representations are shown schematically in Fig. 2. The initial void volume fraction is computed correspondingly as

$$2\text{D (cylindrical):}\quad f_0 = \pi\left(\frac{R_0}{X_0}\right)^2, \qquad 3\text{D (spherical):}\quad f_0 = \frac{4\pi}{3}\left(\frac{R_0}{X_0}\right)^3 \tag{3}$$

where R_0 is the initial void radius and X_0 denotes the center distance, see Fig. 3. A void volume fraction of f_0=1.4% is studied in the following simulations.

In the present model no damage of the intervoid ligaments is incorporated but the matrix material is assumed to be ideal ductile and can undergo arbitrary large deformations. However, at some point the hardening of the material in the intervoid ligament does not compensate the lateral contraction anymore.

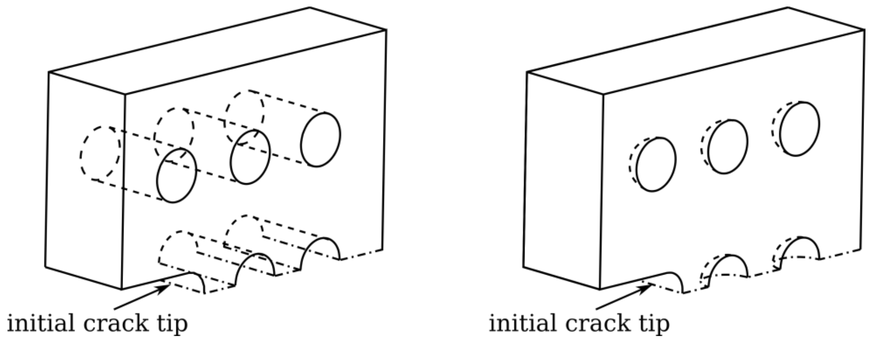

Fig. 2: Spherical and cylindrical voids at the crack tip

Due to this geometrical softening the next ligaments have to carry more load corresponding to an effective crack growth without material separation. In order to quantify this process a measure of relative growth of each void i is introduced as

$$D_i = \frac{W_i - 2R_0}{X_0 - 2R_0} \tag{4}$$

relating the increase of the width W_i of each void to its maximum possible value, see Fig. 3. Correspondingly D_i can take values $0 \le D_\text{i} \le 1$ where $D_\text{i} = 0$ refers to the initial state.

Plotting this value D_i against the position x of each void in the crack plane gives a profile as sketched in Fig. 4. The distance of the center of this profile can be interpreted as amount of effective crack growth. Using the value D_i as weight leads to the definition

$$\Delta a = X_0 \sum_{i=1}^{n} D_i \,. \tag{5}$$

For spherical voids the current extension in x-direction of crack growth is defined as W_i.

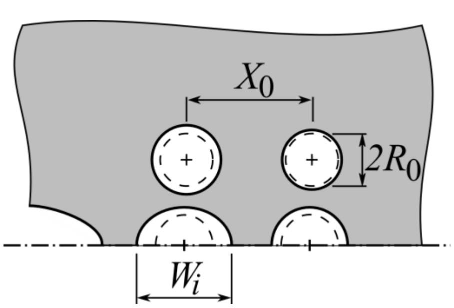

Fig. 3: Evolution of the voids in the ligament

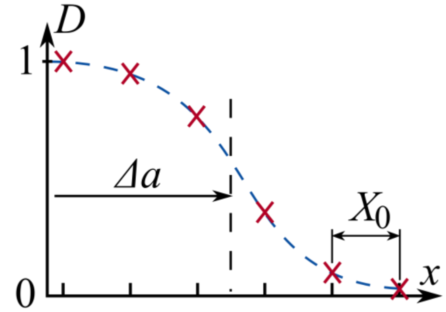

Fig. 4: Crack tip as center oft the softening zone

In order to trace the crack growth a corresponding number of discrete voids needs to employed in the numerical model. In the plane model 60 voids are resolved in direction of crack growth and ten of such layers of voids are incorporated (in the half-model). So many discrete voids cannot be handled with reasonable effort in the 3D model. Therefore, three layers of ten spherical voids each are employed in this case.
The large deformations in the intervoid ligaments require a fine mesh there. A typical employed finite element discretization is shown in Fig. 5. The outer radius of the boundary layer is A_0=4500 X_0 which is much larger than the maximum extent of the plastic zone.

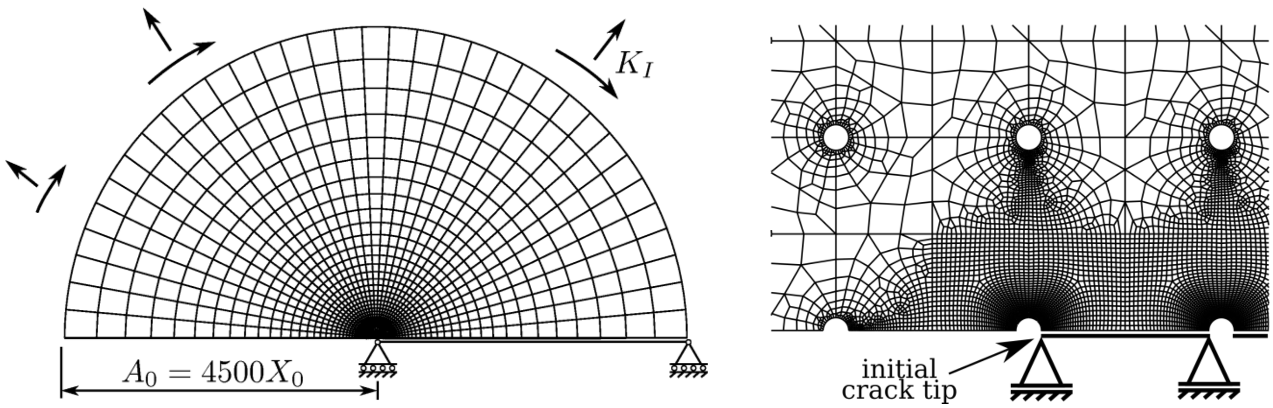

Fig. 5: Mesh of the boundary layer and at the crack tip in the plane model

Results
The evolution of the voids in the process zone is depicted in Fig. 6 for the plane model for two stages of loading. Firstly, the initial crack tip blunts with increasing loading and further voids in the ligament begin to grow (Fig. 6a) before the intervoid ligaments soften and the active softening zone shifts through the ligament (Fig. 6b).
The evolution of the width of the first voids in the crack plane in front of the crack tip with increasing load J is plotted in Fig. 7. It shows that the voids grow subsequently until a limit load J_s is reached at which all voids grow simultaneously. According to the definition (5) of the crack growth as measure of accumulated void growth the crack growth resistance curve in Fig. 8 is obtained.

a)
b)
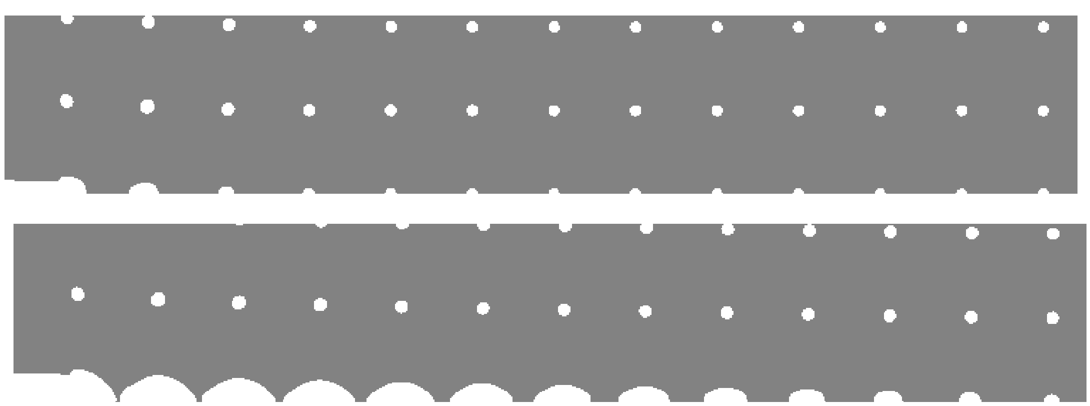

Fig. 6: Process zone a) in the initial region ($J = 0.55\ \sigma_0 X_0$) and b) in the stationary region ($J = 0.96\ \sigma_0 X_0$) for cylindrical voids

The distribution of the void size in the ligament is depicted in Fig. 9 for different load levels. After the initiation stage a stationary profile of the currently active softening zone is formed which shifts congruently along the ligament when the limit load $J=J_s$ is reached. This process is limited in the numerical model by the width of the zone of discrete voids. Fig. 9 shows that this active zone encompasses about 15 voids in the stationary regime. Thus, this number of discrete voids needs to be incorporated in a model in order to reach the stationary state.

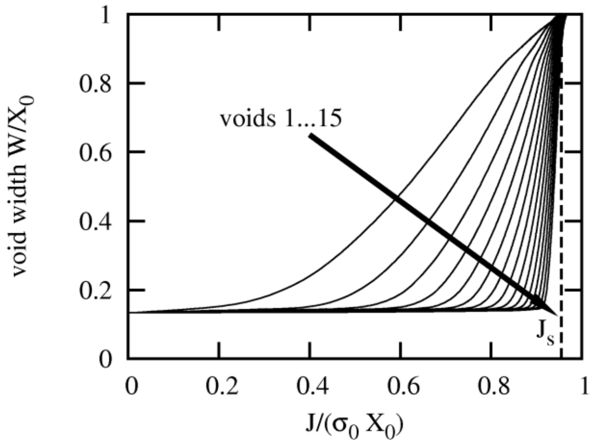

Fig. 7: Evolution of size of the voids in the ligament

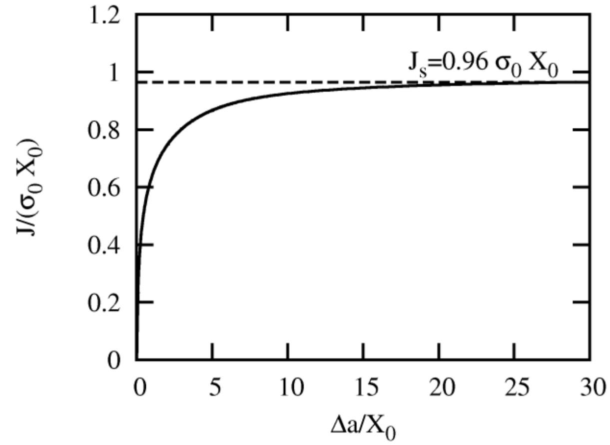

Fig. 8: Crack growth resistance curve

In order to check the influence of the material surrounding the voids a further model is created with discrete voids located in the crack plane only. The material outside this single layer is described either by Mises-plasticity as in literature [7-15] or by the GTN-model. The obtained R-curves are plotted in Fig. 10. The curves show that the crack growth resistance is strongly underestimated if the porosity outside the crack plane is neglected. Apparently, the void growth in the plastic zone prevents the formation of high hydrostatic stresses thus shielding the actual softening zone. In addition, Fig. 10 indicates that the predicted toughness with ten layers of voids (in the half-model) is still larger than with a single layer surrounded by GTN-material. Obviously, the latter does not capture the behavior near the softening zone.

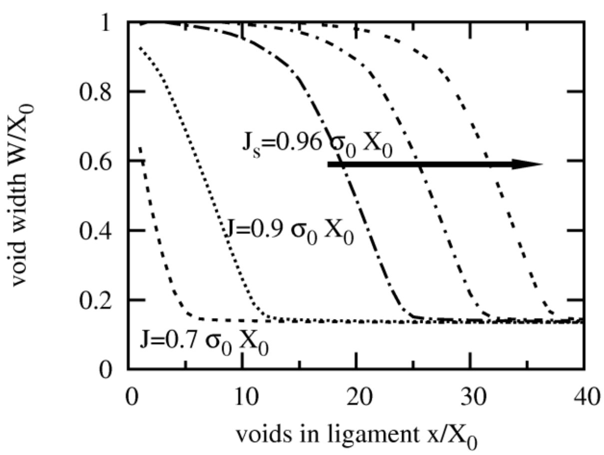

Fig. 9: Void size distribution in the ligament

Further simulations are performed with different numbers of discretely resolved void layers. The plot of the obtained limit load toughness J_s in Fig. 11 indicates that convergence with respect to the number of layers is not reached even with ten layers. However, more layers could not be included due to the big computational effort.

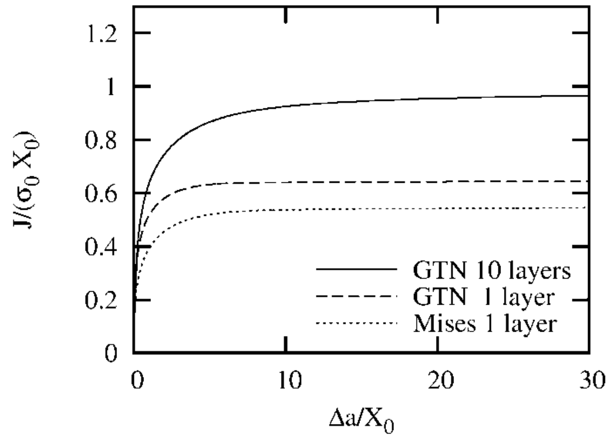

Fig. 10: R-curves for different models of the surrounding material behavior

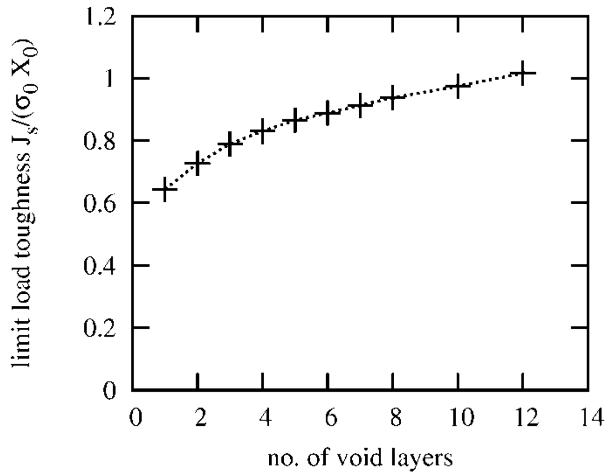

Fig. 11: Influence of the number of resolved void layers

For comparison between the both void representations crack growth resistance curves are plotted in Fig. 12 for the same value of the initial void volume fraction f_0, with cylindrical voids in the plane model and with spherical voids in the three-dimensional model. The results show that the crack growth resistance with the spherical voids has about twice the value of the cylindrical ones. Generally, it is well known that cylindrical voids grow much faster than spherical ones [9-10]. The number of ten discrete voids incorporated in the 3D model until now in direction of crack growth is too small to reach a stationary state as discussed above. Nevertheless, the corresponding limit load J_s can already be estimated as inscribed in the diagram. The immediate increase in the computed R-curve for the spherical voids in Fig. 12 arises when the active softening zone reaches the last discrete void where the zone piles up. As discussed above it is expected that even a larger crack growth resistance will be predicted for spherical voids if more than the currently used three layers of voids are incorporated.

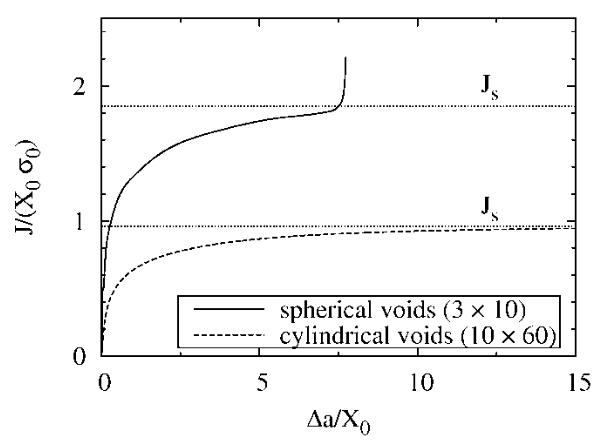

Fig. 12: R-curves for cylindrical and spherical voids

Summary

In the present study the mechanism of ductile crack growth is studied by a micro-mechanical finite-element model. A large number of discrete cylindrical or spherical voids is resolved near the crack tip where steep gradients occur. The voids are taken into account consistently outside this region by means of the GTN-model. A boundary-layer approach is employed to investigate the limit case of a

semi-infinite crack. However, no damage mechanism of the intervoid matrix material is incorporated.
It turns out that the plastic collapse, i.e. the geometrical softening, of the intervoid ligaments is sufficient to induce the movement of the currently active softening zone and the plastic zone at all corresponding to effective crack growth. Due to this mechanism a limit load exists at which the active zone shifts congruently along the crack plane. The width of the active zone in this stationary stage determines the number of discrete voids to be incorporated in a numerical model in order to simulate the collapse behavior and to obtain the related limit load. This minimum number is relatively large compared to the values employed in several studies in the literature. The limit load can be seen as maximum reachable fracture toughness compared to models where additional secondary damage mechanisms are incorporated.
A strong shielding effect due to void growth in the wide region of the plastic zone is observed. So the computed crack growth resistance increases considerable if discrete voids in addition to those in the crack plane are incorporated. A convergence study with respect to the number of layers of voids to be discretely resolved is performed. However, convergence could not be reached until now even with twelve layers of cylindrical voids. This point requires further investigation.
A measure for the current position of the active softening zone is introduced allowing to determine the effective crack length and thus an effective crack growth resistance curve. In accordance with results from literature a larger fracture toughness is predicted with spherical voids compared to a model with cylindrical ones of identical void volume fraction.

Acknowledgement
The financial support by the Deutsche Forschungsgemeinschaft (German Science Foundation) under contracts KU 929/13-2 and KU 929/14-1 is gratefully acknowledged. Furthermore, the authors thank the students A. Burgold and E. Zimmermann for their commitment in performing finite element computations for the present study.

References
[1] A. A. Benzerga and J.-B. Leblond, Adv. Appl. Mech. Vol. 44 (2010), pp. 169-305.
[2] A. L. Gurson, J. Eng. Mater-T. ASME Vol. 99 (1977), pp. 2-15.
[3] V. Tvergaard, Int. J. Fracture. Vol. 17 (1981), pp. 389-407.
[4] V. Tvergaard, Int. J. Fracture Vol. 18 (1982), pp. 237-252.
[5] J. R. Rice and M. A. Johnson, In: *Inelastic Behavior of Solids*, McGraw-Hill, 1970, pp. 641-672
[6] R. M. McMeeking, J. Mech. Phys. Solids. Vol. 25 (1977), pp. 357-381.
[7] S. Aoki, K. Kishimoto, A. Takeya and M. Sakata, Int. J. Fracture Vol. 24 (1984), pp. 267-278.
[8] N. Aravas and R. M. McMeeking, J. Mech. Phys. Solids. Vol. 33 (1985), pp. 25-49.
[9] C. L. Hom and R. M. McMeeking, J. Mech. Phys. Solids.Vol. 37 (1989), pp. 395-415.
[10] J. Kim, X. Gao and T. S. Srivatsan, Int. J. Solids. Struct. Vol. 40 (2003), pp. 7357-7374.
[11] X. Gao, T. Wang and J. Kim, Int. J. Solids. Struct. Vol. 42 (2005), pp. 5097-5117.
[12] V. Tvergaard and J. W. Hutchinson, Int. J. Solids. Struct. Vol. 39 (2002), pp. 3581-3597.
[13] V. Tvergaard, Int. J. Fracture. Vol. 148 (2007), pp. 1-12.
[14] J. P. Petti and J. R. H. Dodds, Int. J. Solids. Struct. Vol. 42 (2005), pp. 3655-3676.
[15] M. Mostafavi, D. Smith and M. Pavier, Comp. Mater. Sci. Vol. 50 (2011), pp. 2759-2770.